Orthogonal planar search (OPS) for coronary artery centerline extraction

Szeling Tang & Chee Seng Chan

Signal, Image and Video Processing

ISSN 1863-1703

SIViP
DOI 10.1007/s11760-014-0746-0

Springer

SIViP
DOI 10.1007/s11760-014-0746-0

ORIGINAL PAPER

Orthogonal planar search (OPS) for coronary artery centerline extraction

Szeling Tang · Chee Seng Chan

Received: 6 February 2014 / Revised: 9 October 2014 / Accepted: 29 December 2014

Abstract In this paper, we investigate orthogonal planar search (OPS) for coronary artery centerline extraction to assist in coronary artery diseases diagnosis. The search mechanism exploits a data-driven algorithm to extract the centerline. Firstly, the best representation of vessel cross section on orthogonal planar is determined. Then, the center of gravity from the crosssection is computed as centerline point iteratively. Branching detection and termination are invoked in this proposed method. We demonstrate the results quantitatively and qualitatively. In addition, we benchmark OPS with three state-of-the-art methods and illustrate the comparison results in radar chart (also known as spider chart). Finally, we discuss limitations of OPS and future works.

Keywords Computed tomography angiography (CTA) · Centerline extraction · Orthogonal

1 Introduction

Over the past years, computed tomography angiography (CTA) has been widely studied for coronary artery diseases (CAD) diagnosis due to its non-invasive imaging procedure and high-quality output images. In CAD diagnosis, the CTA visualization techniques (i.e., volume rendering (VR), maximum intensity projections (MIP), multiplanar reformation (MPR) and curved planar reformation (CPR)) are employed to assist in lumen segmentation, stenosis grading and classification. As a result, coronary artery centerline extraction from CTA is prerequisite for these visualization techniques.

Thus, a reliable coronary artery centerline becomes crucial. Unfortunately, this clinical routine (i.e., extraction of centerline) still heavily dependent on time-consuming manual operations. In this work, an automatic coronary artery centerline extraction is proposed which aims to resolve disadvantages of manual operation by: (1) speed up and ease the reviewing tasks, (2) reduce manual interaction on huge amount of volumetric dataset and (3) decrease inter-operator variability.

Ideally, coronary artery centerline tracking algorithm extracts centerline points from oblique planes, which is orthonormal to the centerline. Nevertheless, tensor perturbation occurred due to (1) numerical errors in its modeling and estimation; and (2) inaccurate interpolation of tiny vessel cross section due to partial volume effect, causing inaccurate centerline extracted. Tang and Chan [1] proposed a neighborhood search feedback algorithm for coronary artery centerline tracking to reduce tracking error propagation. However, the algorithm was immature (i.e., under-track the centerline) to cope with vessel line-like profile and branching problem. Hence, we reckon that extraction of coronary artery from axis source images is insufficient due to vessel's curvature as shown in Fig. 1. As a summary, we identify two main problems:

1. Parts of vessel travel transversely causing insufficient centerline extraction from axis source images.
2. Tensor perturbation and partial volume effect causing inaccurate interpolation of tiny cross section.

As a consequence of these two problems, we propose orthogonal planar search (OPS) for coronary artery centerline extraction from CTA. We assume that orthogonal planars

S. Tang (✉) · C. S. Chan
Center of Image and Signal Processing, Faculty of Computer Science and Information Technology, University of Malaya,
50603 Kuala Lumpur, Malaysia
e-mail: szeling@siswa.um.edu.my

C. S. Chan
e-mail: cs.chan@um.edu.my

Published online: 10 January 2015

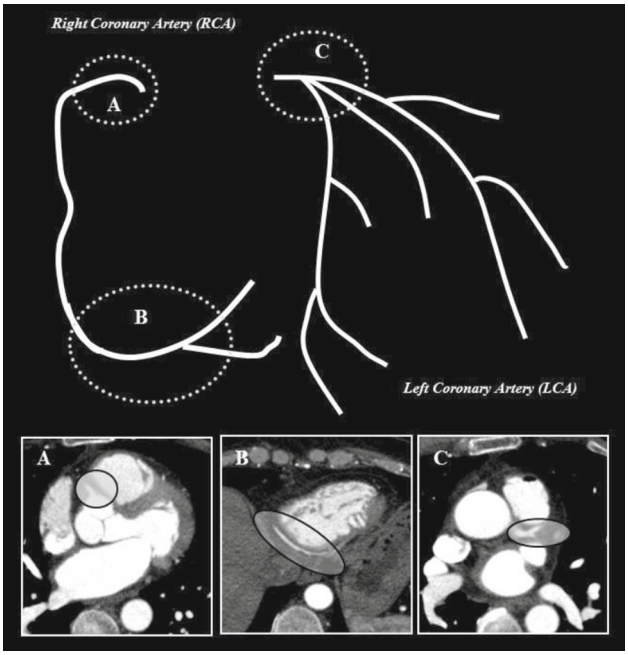

Fig. 1 Parts of vessels travel transversely causing insufficient centerline extraction from axis source images

(i.e., transverse, coronal and sagittal) are sufficient to extract vessels centerline. Due to the complexity of tubular structure, the algorithm required to search for the best representation of vessel cross section from these three orthogonal planars locally. A metric to select the best representation of cross section is required to accomplish OPS (see Sect. 3.3.2). Besides, curvature is an important property to extract vessels. This led us to propose our tracking direction estimation module in order to enhance OPS mechanism (see Sect. 3.4).

For OPS evaluation, we benchmark our proposed method with the three state-of-the-art methods (i.e., Rcadia [2], VRVis [3] and LUMC/Medis [4]) who participated in the centerline extraction challenge of the Rotterdam Coronary Artery Algorithm Evaluation Framework.

This paper is organized as follows: in Sect. 2, we discuss related works in this area and our preliminary experiment. In Sect. 3, we describe the proposed method in detail. In Sect. 4, we show our experimental results and comparison results with state-of-the-art methods. Finally, in Sect. 5, we conclude this paper with discussion and future work.

2 Related works

Coronary artery centerline extraction is challenging due to: (1) image quality is affected by many factors such as spatial and temporal resolution, artefacts due to cardiac motion, (2) high variability of size and curvature, also appearance perturbed by calcifications, stenoses and stents and (3) close to adjacent organs [5].

There are many existing coronary artery centerline extraction algorithms proposed in [5,6] which aim to tackle the aforementioned challenges. Principally, coronary artery centerline extractions are classified into skeleton-based and tracking-based approaches. Skeleton-based approach performs segmentation follow by morphology operations to obtain 3D centerline. Bouraoui et al. [7] anticipated Hit-or-Miss Opening with 13 structure elements to extract coronary artery. This morphology operator is performed on gray-level images instead of binary images. Chen and Molloi [8] proposed an automatic 3D vascular tree construction using 3D morphology operators. The algorithm begins by stacking the CT slices, and then 3D image segmentation is performed follow by 3D thinning to extract the centerline. In order to filter noises (e.g., cycle, stick, non-unit width, spurs etc.) from the thinning process and construct tree concurrently, a simple 3D skeleton pruning and tree construction algorithm is proposed. Xu et al. [9] claimed that the accuracy of coronary artery stenosis detection and quantification is improved after the development of skeletal pruning algorithm on medial axis of arterial tree. On the other hand, tracking-based approach traces vessel centerline with local operators within proximity and track it. For instance, Isola et al. [10] determined relative motion-vector fields (MVF) from phase to phase based on corresponding centerline positions. The full region of interest is extracted from dense MVF by thin plate spline interpolation. Mueller and Maeder [11] used fast-marching minimal paths to extract coronary artery centerline. This is performed after a novel vessel enhancement step in order to avoid the tendency to visit unnecessary pixels.

Skeleton-based approach is claimed to have high-precision approach based on phantom studies [6]. Nevertheless, due to partial volume effect, there are uncertain boundary points problem. Hence, our approach focuses on tracking-based instead of skeleton-based approach.

A standard coronary artery centerline extraction algorithm evaluation framework is proposed by Schaap et al. [12], which is advantageous for comparison of new developed method with state-of-the-art methods as the datasets are publicly provided for benchmarking. Thirteen methods are evaluated in [12]. Majority of the 13 methods proposed minimum cost path as their extraction algorithm [13–23]. Minimum cost path bounds the centerline extraction problem in terms of cost function minimization. A cost function based on proximity likelihood similarity measurement is iteratively minimized. The drawbacks from minimum cost path include possibility to (1) induce exploration of large search space, (2) erroneous shortcut path, (3) defined start and end points are required in order to relax the search mechanism and etc.

The rest of the methods propose model-based or region-growing algorithm to extract centerline. Hoyos et al. [24]

proposed an elastic model to estimate location of potential centerline points. The points iteratively evolve under the action of external force, and internal force untill stability is achieved. Zambal et al. [3] designed two types of cylindrical models; one used to locate seed points of coronary artery and another one used to delineate the vessel. One of the disadvantages from model-based approaches is unfit model to thin and elongated vessel surface. For region-growing algorithm, Kitslaar et al. [25] investigated a combination of fast-marching level set method and backtracking algorithm to obtain a preliminary tree. Then, lumen segmentation is accomplished by delineation of lumen from curved multiplanar reformatted (CMPR) image. In addition, a more precise centerline is extracted from CMPR as well. A work by Yang et al. [4] employed wave propagation (region-growing algorithm) for branch searching on the 'initial tree' (i.e., unconnected branches). Region-growing algorithm fall in the category of greedy algorithm which can be computationally expensive. Thus, we intend to propose a method which avoided the aforementioned drawbacks.

Recently, centerline extraction algorithm evolves into 4D vessel tracking (e.g., [26,27]). Mohan et al. [26] proposed a level set active contour method to extract centerline. They obtain the intensity measurements between the inner disk and the outer annular region by utilize 2D disks directed along the centerline. However, the method is sensitive to initialization, where the seed point must be inside vascular structure which a small tube can be initialized, and it is computationally expensive. Cetin et al. [27] model vessel with 4D curves based on vessel tractography. It is an intensity-based tensor fitting algorithm. The algorithm calculates rank 2 tensor using directional cylinders to trace the path with vessel lumen thickness estimation. In this algorithm, postprocessing is invoked to centralize the centerline due to the vessel's abnormal torsion.

3 Methods

We explore a preliminary experiment to support our aforementioned assumption whereby the orthogonal planars (axial, coronal and sagittal) are sufficient for finding the best representation of cross section along the tubular structure. In particular, we retrieve the orthogonal planars of reference standard centerline based on the principal axis of unit tangent from two consecutive points. We visualize the corresponding planar to validate the best representation of cross sections. Figure 2 clearly shows that the orthogonal planars along the reference standard centerline and each planar contains the best representation of vessels' cross sections.

We define a coronary artery centerline as points extracted from the best representation of cross section on orthogonal planars. Given a volumetric data $\mathbf{V}$, mutually orthogonal

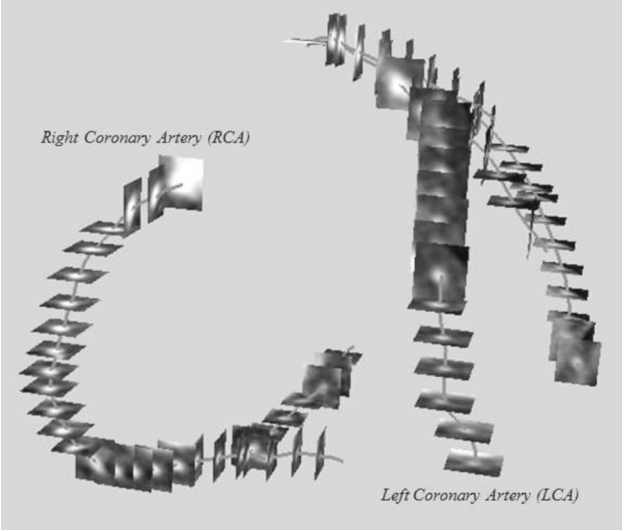

Fig. 2 Best representation of orthogonal planars along reference standard CTA

planar $\mathbf{I}_{\vec{\alpha}} \in \mathbf{V}$ where $\vec{\alpha}$ is unit vector of orthogonal planar in $\mathbb{R}^3$ such that $\mathbf{I}_{(1,0,0)} \rightarrow$ Sagittal, $\mathbf{I}_{(0,1,0)} \rightarrow$ Coronal, $\mathbf{I}_{(0,0,1)} \rightarrow$ Transverse. The planars are explored to extract centerline points, $c(u)$ of centerline, $C(u)$; $u \in [0, L]$ where L is the length of the centerline. $c(u)$ are extracted by analyzing circularity, ω of $\forall$**cc** (connected vessels components) from planar subregions $\mathbf{W}_{\vec{\alpha}} \in \mathbb{R}^2$. Planar subregions ($\mathbf{W}_{\vec{\alpha}}$) are cropped sequentially for processing in order to reduce the computational time.

3.1 Subregions cropping

$\mathbf{W}_{\vec{\alpha}}$ centered by $c_{i-1}(u)$ are cropped prior to image enhancement and define as:

$$\mathbf{W}_{\vec{\alpha}} \in \left\{ \left(\left[R^{\min}_{\vec{\alpha}}, R^{\max}_{\vec{\alpha}} \right], \psi_{\vec{\alpha}} \right) \in \mathbb{R}^2 \times \mathbb{R}^+ \right\} \quad (1)$$

$$R^{\min}_{\vec{\alpha}} = c_{i-1}(u) \cdot (1 - \vec{\alpha}) - w \quad (2)$$

$$R^{\max}_{\vec{\alpha}} = c_{i-1}(u) \cdot (1 - \vec{\alpha}) + w \quad (3)$$

where w is a defined radii vector in $\mathbb{R}^2$ of $\mathbf{W}_{\vec{\alpha}}$. $\psi_{\vec{\alpha}}$ denotes the slice index of orthogonal planar in $\vec{\alpha}$. We present two calculations: one for tracking initialization, another for vessel segment tracking, which will be explained in Sects. 3.3 and 3.4.

3.2 Preprocessing

Herein, we enhance image quality and delineate the connected vessels components (**cc**) for subsequent steps. Conventionally, we apply image smooth filter to improve data points signal such that the outliers are reduced. Standard Gaussian smooth filter $G(x, y) * \mathbf{W}_{\vec{\alpha}}$ is employed, where $G(x, y)$ indicates a 2D Gaussian kernel. Subsequently, a

piecewise function is created to discriminate **cc** from background, i.e., delineate vessel regions from non-blood pool regions. σ, sigma of Gaussian smooth filter controls the blurriness of the image and T_σ is a cut-off variable in the piecewise function which separates vessel regions from background. T_σ is defined empirically. Our algorithm exploits vessels geometric properties in tracking algorithm. Analysis on each **cc** is required. To do this, component connected label technique is performed to label each **cc**.

3.3 OPS in tracking initialization

Generally, a start point inside vessel (i.e., proximal of vessel) is defined for each vessel tree tracking, i.e., right coronary artery (RCA) and left coronary artery (LCA). Nevertheless, this prior information is insufficient for vessel tree tracking due to the complex curvature. Thus, tracking initialization is proposed in order to extract more points to lead the tracking. We emphasize that the best representation of vessel cross section is not on axial source images but is on sagittal or coronal images . This is due to the fact that proximal segments of coronary artery are travel transversely (see Fig. 1).

There are two important factors considered here: (1) evolution direction and (2) feature value.

3.3.1 Evolution direction

Evolution direction of 3D curve tracking is important to indicate current and next position of the curve. However, a defined start point is inefficient to lead the evolution. Thus, all potential evolution directions are investigated to obtain appropriate initial direction using OPS. It can be modeled by combining three orthogonal planars images with voxel-based stepping distance. In particular, two tuple of $\mathbf{W}_{\vec{\alpha}}$, $\prod_{j=0}^{2} \mathbf{W}_{\vec{\alpha}_j^\theta}$ with stepping distance one voxel are extracted using Eq. 1 sequentially for preprocessing where the first tuple is with $\theta = \frac{\pi}{2}$ and second tuple with $\theta = \frac{3\pi}{2}$. We calculate $\psi_{\vec{\alpha}}$ from Eq. 1 as:

$$\psi_{\vec{\alpha}_j^\theta} = c_0(u) \cdot \vec{\alpha}_j + k \sin(\theta) \tag{4}$$

where j is the index of three orthogonal planars. k increases by one in every iteration.

3.3.2 Feature value

We analyze the local geometric property of vascular structure where cross sections of vascular structure are always circular. Circularity, ω of connected vessels component, **cc** is considered as the feature value for tracking initialization and defined as the ratio of cross section perimeter, P to the perimeter of the circle with same area, i.e.,

$$\omega_b = \frac{P_b}{2\sqrt{\pi \cdot A_b}} \tag{5}$$

P can be estimated by any edge detection algorithm. Herein, we use morphology operators to achieve this prupose. A denotes the area of cross section, i.e., pixels count of cross sections and b is index of **cc**. In our work, we empirically define $0.8 \leq \omega_b \leq 1.0$ as sufficient circularity of vessel cross sections (i.e., the best representation of vessels cross section). All **cc** from preprocessing are validated and tracking initialization point is extracted from corresponding cross section.

3.4 OPS in vessel segment tracking

In order to perform CAD diagnosis from the CTA, experts are required to study CTA dataset by rotating orthogonal planar and identify the coronary artery conditions. This is a tedious process which may take up to few hours. Thus, an automated system is more essential for the experts. In order to automate this process, the algorithm must able to transform in between transverse, coronal and sagittal. According to the preliminary experiment (see Fig. 2), we propose OPS, by utilizing the orthogonal planars from volume data for processing. Sequential decision is invoked to optimize the algorithm. Instead of generating two tuples of orthogonal planars as in Sect. 3.3, we now determine current planar, $\vec{\alpha}_i$ by exploiting the continuity of curvature to predict next potential orthogonal planar. From tracking initialization in Sect. 3.3, two initial points inside vessels are extracted. Thus, $\vec{\alpha}_i$ is predictable based on angle, ϕ which in between unit tangent, $\vec{\tau} = \frac{c_0^n(u)\vec{c_{i-1}}(u)}{|c_0^n(u)c_{i-1}(u)|}$ and $\vec{\beta}$ where $\vec{\beta} \perp \vec{\alpha}_i$ (see left figure in Fig. 3).

$c_0^n(u)$ indicates the initial points of each linear segment, n denotes the index of segments. Note that $c_0^n(u)$ is updated when the orthogonal planar changed. As consider the continuity of curvature, no sharp turning point of the curve is observed. When $\phi \geq T_\phi$, turning point is identified and $\vec{\alpha}_i$ is determined by selecting the principal axis of $\vec{\tau}$ (see Eq. 7). Next, we crop $\mathbf{W}_{\vec{\alpha}_i}$ from planar $\vec{\alpha}_i$ by Eq. 1 and calculate ψ_i using below equation:

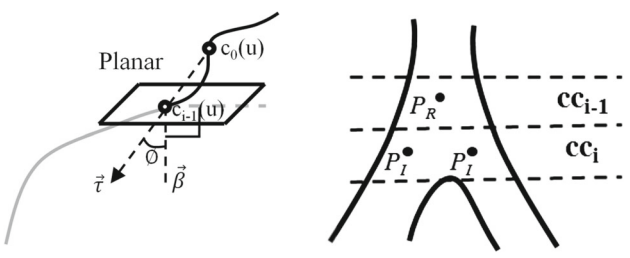

Fig. 3 *Left* angle ϕ in between unit tangent of centerline ($\vec{\tau}$) and unit vector orthogonal to planar ($\vec{\beta}$). $c_0^n(u)$ is updated when orthogonal planar changed. *Right* branching detection

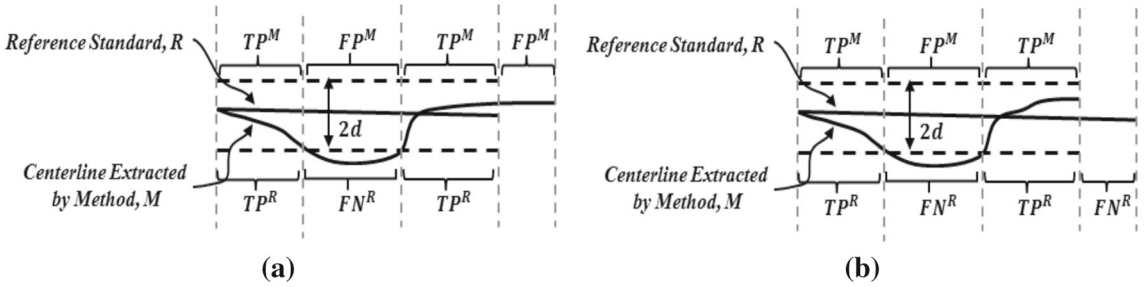

Fig. 4 $\mathrm{TP^M}$, $\mathrm{TP^R}$, $\mathrm{FP^M}$ and $\mathrm{FN^R}$ when **a** the evaluated centerline is elongated more than the reference standard and **b** reference standard elongated more than the evaluated centerline

$$\psi_i = c_{i-1}(u) \cdot \vec{\alpha}_i + \frac{\max(\vec{\tau})}{|\max(\vec{\tau})|} \tag{6}$$

where

$$\vec{\alpha}_i = \begin{cases} (1,0,0), & \text{if } \max(\vec{\tau}) \text{ is } \mathbf{x} \text{ axis} \\ (0,1,0), & \text{if } \max(\vec{\tau}) \text{ is } \mathbf{y} \text{ axis} \\ (0,0,1), & \text{if } \max(\vec{\tau}) \text{ is } \mathbf{z} \text{ axis.} \end{cases} \tag{7}$$

Subsequently, preprocessing (see Sect. 3.2) is performed on determined orthogonal planar. Center of gravity, CoG from the corresponding **cc** is extracted as current centerline point, $c_i(u)$. However, false positive may occurred and the tracking leaks to other adjacent structure. Thus, we extract alternative orthogonal planars at $c_{i-1}(u)$ if no **cc** from orthogonal planar $\vec{\alpha}_i$ to resolve the problems. The alternative planars $\vec{\alpha}_a$ consist of other two orthogonal planars. $\forall$**cc** from planars $\vec{\alpha}_a$ are validated sequentially to reduce computational power. We implement a multiscale vessel segment tracking where vessel segment tracking (in Sect. 3.4) is performed iteratively with various σ in preprocessing (see Sect. 3.2) to obtain the best representation of cross section.

3.5 Branching detection

In order to handle the vessels branching problem, we analyze $\forall$**cc** to detect root of branch, P_R and initial of branch, P_I. In particular, we detect P_I where **cc** with $\mu \geq 1.8$; μ is ratio of width and height of **cc**, we compute at least two points from **cc** and mark it. The P_R is determined where $\mathbf{cc}_{i-1}$ with single point extracted and $\mathbf{cc}_i$ with more than one point extracted (see right figure in Fig. 3). Subsequently, each pair of P_R and P_I is assigned as input to vessel segment tracking (in Sect. 3.4).

4 Experimental results and discussion

We evaluate the performance of proposed method on 18 datasets which publicly available for MICCAI segmentation challenge 2012, "3D Segmentation In The Clinic: A Grand Challenge". The CTA dataset are acquired with average resolution 0.38 mm × 0.38 mm × 0.37 mm. Prior to the evaluation, correspondence between the points of reference standard and the points from each method is identified. Subsequently, true positive, false positive and false negative are labeled on the points based on correspondence points (see Fig. 4a, b).

Evaluation 1: A point of the reference standard is labeled as true positive, $\mathrm{TP^R}$ if the Euclidean distance to at least one of the connected points on the evaluated centerline is less than defined distance, d and false negative, $\mathrm{FN^R}$ otherwise.

Evaluation 2: A point of the evaluated centerline is labeled as true positive, $\mathrm{TP^M}$ if the Euclidean distance from at least one of the connected points on the reference standard CTA is less than d and false positive, $\mathrm{FP^M}$ otherwise.

Here, d is equal to 0.75 mm because we only consider the vessels which are assumed to be clinically relevant, i.e., vessels diameter ≈1.5 mm or larger according to [28]. Two measures were used in our evaluations:

(1) *Overlaping* (V_c) represents the ability to track the complete vessel annotated from CTA with a measure similar to Dice coefficient and defined as

$$V_\mathrm{c} = \frac{\mathrm{TP^M} + \mathrm{TP^R}}{\mathrm{TP^M} + \mathrm{TP^R} + \mathrm{FP^M} + \mathrm{FP^R}} \tag{8}$$

(2) *Average distance* (D_c) indicates the average distance of all the connections between the CTA reference standard and the evaluated centerline given that the connections have Euclidean distance smaller than d.

We compare our proposed method and centerlines extracted by the results from the three teams (i.e., Rcadia team [2], VRVis team [3] and LUMC/Medis team [4]) with CTA reference standard. Table 1 shows the comparison results of V_c and D_c. According to Table 1, our proposed method (OPS) achieved an average 80 % in V_c and an average 0.42 mm in D_c. Figure 5 shows some examples of the superimposed

Table 1 Comparison results for V_c and D_c

Methods	V_c						D_c					
	RCA			LCA			RCA			LCA		
	Min. (%)	Max. (%)	Avg. (%)	Min. (%)	Max. (%)	Avg. (%)	Min. (mm)	Max. (mm)	Avg. (mm)	Min. (mm)	Max. (mm)	Avg. (mm)
Rcadia team [2]	55.2	98.9	91.6	71.0	98.3	90.6	0.28	0.40	0.34	0.30	0.39	0.34
VRVis team [3]	72.7	97.8	90.7	85.1	94.9	92.0	0.30	0.44	0.35	0.29	0.40	0.33
LUMC/Medis team [4]	49.5	95.9	86.0	74.6	95.1	87.4	0.32	0.51	0.40	0.29	0.44	0.37
OPS	44.6	90.9	79.5	59.8	93.2	80.5	0.36	0.52	0.42	0.34	0.54	0.41

(a) Dataset 1 **(b)** Dataset 2 **(c)** Dataset 3

Fig. 5 Superimpose of evaluated centerline (from our proposed OPS) in *white* and reference standard in *black* from three dataset

images of the results from our proposed method (in white dots) and reference standard CTA (in black lines). Observe that subimages from Fig. 5, generally the results are acceptable. Unfortunately, some noise occurred or centerline tracking failed mainly at the end of vessels. The reasons of poor accuracy from OPS compare to the state-of-the-art methods are:

- The tiny connected vessel component (**cc**) vanish during preprocessing step, especially at distal of vessel and branches.
- Improper branching detection rules (see Sect. 3.5).

However, herein we proposed a new strategy where centerline tracking approach is based on an orthogonal planar search mechanism.

4.1 Comparison with the state-of-the-art methods

We compare the functionality of OPS with three state-of-the-art methods, the selection of relevant performance indicators is crucially important to provide informative comparison, and the indicators must be measurable features such that ranking can be assigned to the comparators. Thus, we select the following indicators in order to highlight certain beneficial features of our OPS:

1. *Simplicity*—estimate based on the complexity of each stage in the algorithm.
2. *Flexibility*—consider number of models invoked, supervised or unsupervised algorithm, amount of interaction, e.g., number of start points or end points required, etc.
3. *Robustness*—based on the amount of undetected vessels compare to reference CTA.
4. *Accuracy*—the average overlapping (V_c) from extracted centerline and reference CTA, see Table 1.
5. *Erroneous*—the average distance (D_c) between extracted centerline and reference CTA, see Table 1.

Table 2 summarizes the comparison of OPS with three comparators based on the indicators with ranking. Figure 6 demonstrates the comparison ranking in spider chart to provide a better understanding. As highlighted here, the *Accuracy* and *Erroneous* are the results extracted from Table 1 where the OPS underperformed when compared to other comparators. Despite these, we discuss other features which reveal the strength of OPS. Notice that our proposed method ranked first in *Simplicity* and *Flexibility*. In particular, our

Table 2 Comparison of OPS with state-of-the-art methods

Methods	Comparison/ranking									
	Simplicity		Flexibility		Robustness		Accuracy (mm)		Erroneous (%)	
Rcadia [2]	Obtain binary image. Get distance map. Add identified end points to the graph. Centerline backtracking from identified end points untill root	2	End points are identified prior to vessel tracking	2	RCA and LCA are extracted from all dataset	1	0.337	1	92.1	1
VRVis [3]	Estimate vesselness. Approximate direction. Tracking based on direction. Apply Depth-first-search to explore branching	3	Two types of models are designed for algorithm	4	3 RCAs undetected from all dataset	4	0.342	2	91.4	2
LUMC/Medis [4]	Perform multiscale vesselness. Extract initial tree by component connected labeling and skeletonization. Use wave propagation in branch search. Refine centerline by straightened MPR	4	Supervised wave propagation	3	1 RCA undetected from all dataset	2	0.39	3	86.7	3
OPS	Perform preprocessing on cropped image. Obtain connected vessel components. OPS for vessel initialization. OPS for vessel segments tracking	1	Non-model and unsupervised method	1	2 LCA undetected from all dataset	3	0.42	4	80.0	4

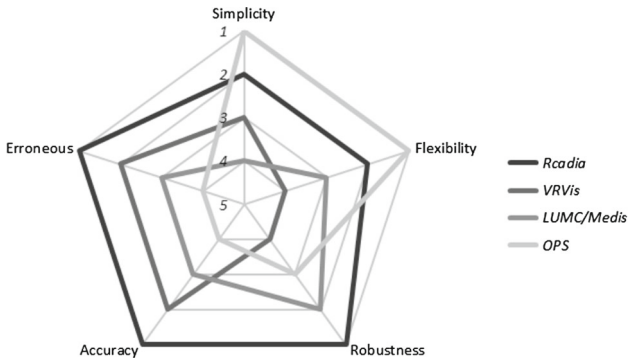

Fig. 6 Spider chart of comparison between OPS with state-of-the-art methods

proposed method freely uses advanced mathematical algorithms to solve the problems based on logical theory without sophisticated processes. In fact, this support the results from Table 1 in which OPS slightly underperformed compared to others.

5 Conclusion and future works

In this work, we investigated the performance of OPS based on our earlier assumption (in Fig. 2). For evaluation, we benchmark OPS with three groups of centerline algorithm, which provide promising results. Notice that OPS performed V_c with variance in between 6.7 and 11.4 % and D_c with variance in between 0.03 and 0.08 mm compare with the three teams. It can been seen in Fig. 5 that OPS tracks the centerline quite well at the beginning but noise occurred at the end of the centerline. Nevertheless, our proposed method can be replicated easily due to its simplicity and flexibility (see Table 2; Fig. 6). In conclusion, while OPS has its limitations, but it is a new strategy for 3D centerline tracking from volumetric data.

In future works, we target to resolve the two main limitations aforementioned (see Sect. 4). First, we plan to integrate multiscale preprocessing to enhance the connected vessel components. Second, we will investigate a robust branching detection algorithm to the extract entire vessel tree.

References

1. Tang, S., Chan, C.S.: A neighbourhood search feedback for coronary artery centerline tracking. In: MVA2013 IAPR International Conference on Machine Vision Applications, pp. 85–88, May 20–23 (2013)
2. Goldenberg, R., et al.: Computer-aided simple triage (CAST) for coronary CT angiography (CCTA). Int. J. Comput Assist. Radiol. Surg. **7**(6), 819–827 (2012)
3. Zambal, S., Hladuvka, J., Kanitsar, A., Bühler, K.: Shape and appearance models for automatic coronary artery tracking. In: MICCAI Workshop Grand Challenge Coronary Artery Tracking, The MIDAS Journal. http://hdl.handle.net/10380/1420 (2008). Accessed 9 Dec 2010
4. Yang, G., et al.: Automatic centerline extraction of coronary arteries in coronary computed tomographic angiography. Int. J. Cardiovasc. Imaging **28**(4), 921–933 (2012)
5. Lesage, D., Angelini, E.D., Bloch, I., Funka-Lea, G.: A review of 3D vessel lumen segmentation techniques: models, features and extraction schemes. Med. Image Anal. **13**(6), 819–845 (2009)
6. Kirbas, C., Quek, F.: A review of vessel extraction techniques and algorithms. ACM Comput. Surv. **36**(2), 81–121 (2004)
7. Bouraoui, B., Ronse, C., Baruthio, J., Passat, N., Germain, P.: 3D segmentation of coronary arteries based on advanced mathematical morphology techniques. Comput. Med. Imaging Graph. **34**(5), 377–387 (2010)
8. Chen, Z., Molloi, S.: Automatic 3D vascular tree construction in CT angiography. Comput. Med. Imaging Graph. **27**(6), 469–479 (2003)
9. Xu, Y., Liang, G., Hu, G., Yang, Y., Geng, J., Saha, P.K.: Quantification of coronary arterial stenoses in CTA using fuzzy distance transform. Comput. Med. Imaging Graph. **36**(1), 11–24 (2012)
10. Isola, A., Metz, C., Schaap, M., Klein, S., Grass, M., Niessen, W.J.: Cardiac motion-corrected iterative cone-beam CT reconstruction using a semi-automatic minimum cost path-based coronary centerline extraction. Comput. Med. Imaging Graph. **36**(3), 215–226 (2012)
11. Mueller, D., Maeder, A.: Robust semi-automated path extraction for visualising stenosis of the coronary arteries. Comput. Med. Imaging Graph. **32**(6), 463–475 (2008)
12. Schaap, M., Metz, C., van Walsum, T., van der Giessen, A., Weustink, A., Mollet, N., Bauer, C., Bogunovi, H., Castro, C., Deng, X., Dikici, E., O'Donnell, T., Frenay, M., Friman, O., Hoyos, M., Kitslaar, P., Krissian, K., Khnel, C., Luengo-Oroz, M., Orkisz, M., Smedby, O., Styner, M., Szymczak, A., Tek, H., Wang, C., Warfield, S., Zambal, S., Zhang, Y., Krestin, G., Niessen, W.: Standardized evaluation methodology and reference database for evaluating coronary artery centerline extraction algorithms. Med. Image Anal. **13**(5), 701–714 (2009)
13. Bauer, C., Bischof, H.: Edge based tube detection for coronary artery centerline extraction. In: MICCAI Workshop Grand Challenge Coronary Artery Tracking, The MIDAS Journal. http://hdl.handle.net/10380/1403 (2008). Accessed 9 Dec 2010
14. Castro, C., Luengo-Oroz, M., Santos, A., Ledesma-Carbayo, M.: Coronary artery tracking in 3D cardiac CT images using local morphological reconstruction operators. In: MICCAI Workshop Grand Challenge Coronary Artery Tracking, The MIDAS Journal. http://hdl.handle.net/10380/1436 (2008). Accessed 9 Dec 2010
15. Dikici, E., O'Donnell, T., Grady, L., Setser, R., White, R.D.: Coronary artery centerline tracking using axial symmetries. In: MICCAI Workshop Grand Challenge Coronary Artery Tracking, The MIDAS Journal. http://hdl.handle.net/10380/1425 (2008). Accessed 9 Dec 2010
16. Friman, O., Kühnel, C., Peitgen, H.-O.: Coronary centerline extraction using multiple hypothesis tracking and minimal paths. In: MICCAI Workshop Grand Challenge Coronary Artery Tracking, The MIDAS Journal. http://hdl.handle.net/10380/1433 (2008). Accessed 9 Dec 2010
17. Gülsün, M.A., Tek, H.: Robust vessel tree modeling. In: Medical Image Computing and Computer-Assisted Intervention—MICCAI, pp. 602–611. Springer (2008)
18. Krissian, K., Bogunovic, H., Pozo, J., Villa-Uriol, M., Frangi, A.: Minimally interactive knowledge-based coronary tracking in CTA using a minimal cost path. In: MICCAI Workshop Grand Challenge Coronary Artery Tracking, The MIDAS Journal. http://hdl.handle.net/10380/1435 (2008). Accessed 9 Dec 2010
19. Metz, C., Schaap, M., Van Walsum, T., Niessen, W.: Two point minimum cost path approach for CTA coronary centerline extraction. In: MICCAI Workshop Grand Challenge Coronary Artery Tracking, The MIDAS Journal. http://hdl.handle.net/10380/1510 (2008). Accessed 9 Dec 2010
20. Szymczak, A.: Vessel tracking by connecting the dots. In: MICCAI Workshop Grand Challenge Coronary Artery Tracking, The MIDAS Journal. http://hdl.handle.net/10380/1406 (2008). Accessed 9 Dec 2010
21. Tek, H., Gulsun, M.A., Laguitton, S., Grady, L., Lesage, D., Funka-Lea, G.: Automatic coronary tree modeling. In: MICCAI Workshop Grand Challenge Coronary Artery Tracking, The MIDAS Journal. http://hdl.handle.net/10380/1426 (2008). Accessed 9 Dec 2010
22. Wang, C., Smedby, Ö.: Coronary artery segmentation and skeletonization based on competing fuzzy connectedness tree. In: Medical Image Computing and Computer-Assisted Intervention—MICCAI, pp. 311–318. Springer (2007)
23. Zhang, Y., Chen, K., Wong, S.: 3D interactive centerline extraction. In: MICCAI Workshop Grand Challenge Coronary Artery Tracking, The MIDAS Journal. http://hdl.handle.net/10380/1417 (2008). Accessed 9 Dec 2010
24. Hoyos, M.H., Zuluaga, M.A., Lozano, M., Prieto, J.C., Douek, P.C., Magnin, I.E., Orkisz, M.: Coronary centerline tracking in CT images with use of an elastic model and image moments. In: MICCAI Workshop Grand Challenge Coronary Artery Tracking, The MIDAS Journal. http://hdl.handle.net/10380/1401 (2008). Accessed 9 Dec 2010
25. Kitslaar, P.H., Frenay, M., Oost, E., Dijkstra, J., Stoel, B., Reiber, J.H.: Connected component and morpholgy based extraction of arterial centerlines of the heart (cocomobeach). In: MICCAI Workshop Grand Challenge Coronary Artery Tracking, The MIDAS Journal. http://hdl.handle.net/10380/1460 (2008). Accessed 9 Dec 2010
26. Mohan, V., Sundaramoorthi, G., Tannenbaum, A.: Tubular surface segmentation for extracting anatomical structures from medical imagery. IEEE Trans. Med. Imaging **29**(12), 1945–1958 (2010)
27. Cetin, S., Demir, A., Yezzi, A., Degertekin, M., Unal, G.: Vessel tractography using an intensity based tensor model with branch detection. IEEE Trans. Med. Imaging **32**(2), 348–363 (2013)
28. Leschka, S., et al.: Accuracy of MSCT coronary angiography with 64-slice technology: first experience. Eur. Heart J. **26**(15), 1482–1487 (2005)